

# 1

## Emission and Excitation Mechanisms of Phosphors

Cees R. Ronda

### 1.1

#### Introduction

In this chapter, basic concepts involved in luminescence will be discussed. We will take a closer look at a number of excitation mechanisms which are involved in generating luminescence and processes which lead to luminescence, taking illustrative examples from luminescent materials applied in fluorescent lamps and cathode ray tubes. With respect to fluorescent lamps, we will restrict ourselves to discharge lamps based on the low-pressure Hg discharge. Other applications will be treated more extensively in separate chapters. A separate chapter in this book is devoted to scintillators, used in medical detectors. Here the excitation mechanism strongly resembles the one in cathode ray phosphors. Phosphors for Light-Emitting Diodes (LEDs) and phosphors for Plasma Display Panels (PDPs) are treated separately as well, the processes leading to excitation and emission being comparable to those in fluorescent lamps.

Possible ways to influence the emission color will be discussed, this being of strong relevance for applications. We will also give an overview of the most popular devices that rely on luminescent materials, and finally we will touch upon processes that result in nonradiative recombination.

Recently, organic luminescent materials have attracted considerable interest in view of their application in organic light-emitting diodes. In this chapter, however, we discuss inorganic phosphors only.

### 1.2

#### General Considerations – Fluorescent Lamps

On passing a current through an Hg discharge, UV light is generated as a consequence of electronic transitions on the Hg atoms. In low-pressure Hg discharge, the main emission line is located at 254 nm. This light is invisible and harmful; therefore it has to be converted into visible light. This is done by the application of luminescent materials. These materials have to show a strong absorption at 254 nm and have to convert this into visible light very efficiently. In most of the fluorescent lamp phosphors, the optical

processes leading to luminescence do not involve host lattice states, implying that the energy gap is at least 4.9 eV, this being the energy of a photon with wavelength 254 nm. Therefore, the luminescent materials applied in fluorescent lamps are insulators.

The conversion efficiency of luminescent materials is very high: about 90 % of the UV photons are absorbed, and also about 90 % of the absorbed photons are converted into visible light. This implies that such materials cannot be improved any further in terms of conversion efficiency unless materials can be found that generate more than one visible photon after absorption of a UV photon. This is the subject of a separate chapter in this book.

An elementary calculation shows that, even though fluorescent lamps are the most efficient white light sources, the overall energy efficiency is nevertheless rather limited: only about 25 %. The percentage energy efficiency is calculated as follows:

$$\eta = \eta_{\text{disch}} \cdot \eta_{\text{phos}} \cdot (254/550) \cdot 100 \quad (1)$$

in which 254 nm is the wavelength of the exciting Hg radiation in nm and 550 nm is the mean wavelength of the light emitted. As in current fluorescent lamp phosphors only one visible photon per absorbed UV photon is generated, the difference in photon energy represents energy loss. The discharge efficiency ( $\eta_{\text{disch}}$ ) of the Hg discharge is about 70 % and the conversion efficiency ( $\eta_{\text{phos}}$ ) of the phosphors (on a photon basis) is about 80 %. Insertion of these numbers leads to the overall efficiency of about 25 %. In view of the very high Hg discharge efficiency, here also hardly any significant improvement can be expected. This implies that this lamp concept has reached physical limits in terms of energy efficiency.

Compact fluorescent lamps have a lower light generation efficiency (only 15 %). As the luminescent materials applied are the same or very similar, this must be due to the lower discharge efficiency in these devices, which, in turn, is due to the smaller diameter of the lamp envelope and therefore to the increased wall losses: excited Hg atoms reach the ground state on interacting with the lamp wall without generating UV light: energy and momentum can be conserved by interaction of excited species with the wall without generation of light.

### 1.3

#### General Considerations – Cathode Ray Tubes

Though the importance of cathode ray tubes is rapidly decreasing, we will treat the luminescence mechanism in these materials in view of its historical importance. In addition, the excitation mechanism that comprises excitation with high-energy particles (electrons, X-ray photons, or  $\gamma$ -rays) is also operative in phosphors used in scintillators for, e.g., medical applications.

Luminescent materials applied in cathode ray tubes in general differ from those applied in fluorescent lamps. Excitation proceeds via the band gap. To achieve high efficiencies, small values for the band gap are needed, as will be elucidated below. For this reason, quite a few luminescent materials applied in cathode ray tubes are semiconductors.

The luminescence mechanism operating in the blue and green emitting phosphors applied in cathode ray tubes is a beautiful example of luminescence involving defect states in semiconductors. We will therefore also discuss this mechanism in some detail.

The maximum energy efficiency of the cathode ray phosphors is relatively low, at most about 25 %, as will be outlined in this chapter. Also for these phosphors, the maximum efficiencies have been reached.

In the next sections, we will deal with luminescence and excitation mechanisms.

## 1.4 Luminescence Mechanisms

Luminescent materials, also called phosphors, are mostly solid inorganic materials consisting of a host lattice, usually intentionally doped with impurities (see Fig. 1.1). The impurity concentrations generally are low in view of the fact that at higher concentrations the efficiency of the luminescence process usually decreases (concentration quenching, see below). In addition, most of the phosphors have a white body color. Especially for fluorescent lamps, this is an essential feature to prevent absorption of visible light by the phosphors used. The absorption of energy, which is used to excite the luminescence, takes place by either the host lattice or by intentionally doped impurities. In most cases, the emission takes place on the impurity ions, which, when they also generate the desired emission, are called activator ions. When the activator ions show too weak an absorption, a second kind of impurities can be added (sensitizers), which absorb the energy and subsequently transfer the energy to the activators. This process involves transport of energy through the luminescent materials. Quite frequently, the emission color can be adjusted by choosing the proper impurity ion, without changing the host lattice in which the impurity ions are incorporated. On the other hand, quite a few activator ions show emission spectra with emission at spectral positions which are hardly influenced by their chemical environment. This is especially true for many of the rare-earth ions.

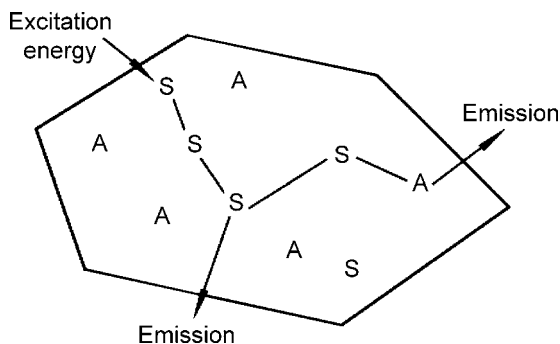


**Fig. 1.1** Luminescent material containing activator ions A (ions showing the desired emission) and sensitizing ions S (on which, e.g., UV excitation can take place).

## 1.4.1

**Center Luminescence**

In the case of center luminescence, the emission is generated on an optical center, in contradiction to, e.g., emission, which results from optical transitions between host lattice band states or from a transition between two centers. Such an optical center can be an ion or a molecular ion complex.

One speaks of characteristic luminescence when, in principle, the emission could also occur on the ion in a vacuum, i.e. when the optical transition involves electronic states of the ion only. Characteristic luminescence can consist of relatively sharp emission bands (spectral width typically a few nm), but also of broad bands, which can have widths exceeding 50 nm in the visible part of the spectrum. Broad emission bands are observed when the character of the chemical bonding in the ground and excited state differs considerably. This goes hand in hand with a change in equilibrium distance between the emitting ion and its immediate chemical environment and is commonly explained with the configuration coordinate diagram (Fig. 1.2).

In this diagram,  $Q_g$  and  $Q_e$  represent the metal-ligand distances in the ground and excited states, respectively.  $E_a$  and  $E_e$  are the energies at which the absorption and emission bands have their maximum intensity, respectively.  $\Delta$  is the energy of the so-called zero phonon line; this transition involves completely relaxed excited and ground states, and no excited phonon states are involved – hence the name of this kind of transitions. The phonon frequencies in the ground and excited state are given by  $\hbar\omega_g$  and  $\hbar\omega_e$ , respectively. The relaxation energies in the ground and excited states can be expressed as a product of the phonon energy and the so-called Huang-Rhys factors. The Huang-Rhys factors  $S_e$  and  $S_g$  in the ground and excited state (being pure numbers), respectively, give the mean number of phonons involved in the absorption and emission processes, respectively. In the harmonic approximation, the curvature of the parabolic band (determined by the bond strength), the phonon frequencies, and the Huang-Rhys factors are the same in the ground and excited state. This picture

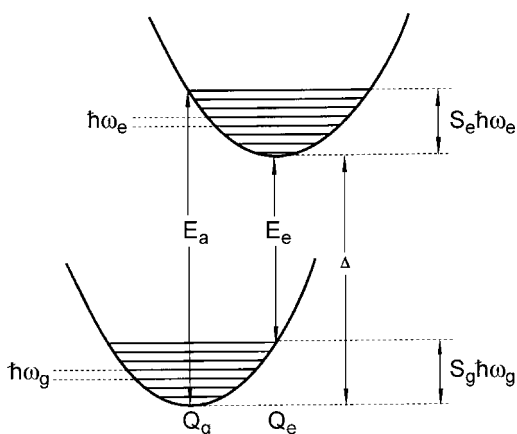


**Fig. 1.2** Configurational coordinate diagram.

is very elementary. For example, it does not describe thermal expansion of the lattice. However, it does give a lot of insight. It can, e.g., be used in showing that a larger Stokes Shift is expected on increasing lattice relaxation and also in the description of thermal quenching of the emission (see further below).

Broad bands are observed for many optical transitions in the partly filled d-shell of transition metal ions ( $d \rightarrow d$  transitions), but also for transitions between the 5d shell and the 4f shell of rare-earth ions ( $d \rightarrow f$  transitions) and for emission on  $s^2$  ions (these ions possess a “lone pair” of s electrons), like  $Tl^+$ ,  $Pb^{2+}$ , or  $Sb^{3+}$ . Sharp emission bands are characteristic of optical transitions between electronic states with chemical bonding character (almost) the same for ground and excited state, and for the same reason also of optical transitions between electronic states that hardly participate in the chemical bonding (e.g.,  $f \rightarrow f$  transitions on rare-earth ions).

In the case of optical processes involving electronic states which participate in the chemical bonding, the nature of the bonding (covalent, ionic) and the symmetry of the site at which the emitting ion is incorporated play a very important role. This is generally described by the ligand field theory, which we do not treat here. We will use the term symbols for the description of the electronic transitions which arise from the site symmetry of the ions of interest, however.

An example of a broad  $d \rightarrow d$  emission band (in the green part of the spectrum) is the emission of  $Mn^{2+}$  in  $BaMgAl_{10}O_{17}$ : Eu, Mn, see Fig. 1.3.

The green emission is generated by a  $d \rightarrow d$  optical transition on the  $Mn^{2+}$  ion with high spin  $d^5$  electronic configuration (all electrons have their spin oriented in the same direction). The optical transition leading to emission is  ${}^4T_{1g} \rightarrow {}^6A_{1g}$ . The electronic configurations in the ground and excited state are  $(t_{2g})^3 (e_g)^2$  and  $(t_{2g})^4 (e_g)^1$ , respectively. The emission generated reflects how the optical properties of the ion depend on its chemical environment. This luminescent material can be applied as green phosphor in very high-quality fluorescent lamps and also in plasma display

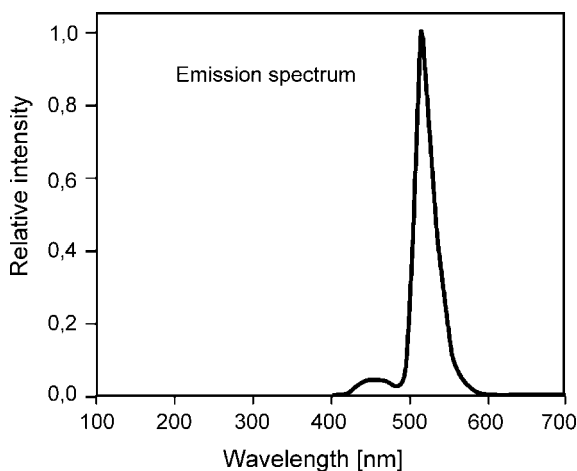


Fig. 1.3  $Mn^{2+}$  emission in  $BaMgAl_{10}O_{17}$ :Eu,Mn.

panels. Its quantum efficiency is very high (90 %), and it shows a very good absorption at 254 nm, the absorption taking place on the  $\text{Eu}^{2+}$  ion, followed by energy transfer to  $\text{Mn}^{2+}$ . This process is elucidated further below. The composition without  $\text{Mn}^{2+}$  shows efficient blue  $\text{Eu}^{2+}$  emission; this emission is responsible for the shoulder at 450 nm and is used as blue emitting phosphor in high-quality fluorescent lamps. The emission stems from the optically allowed  $5d-4f$  transition on  $\text{Eu}^{2+}$ , which is consequently very fast (decay time about 1  $\mu\text{s}$ ).  $\text{Sr}_5(\text{PO}_4)_3\text{Cl}:\text{Eu}$  shows virtually the same emission band, and is used in high-quality fluorescent lamps as well.

An example of  $d \rightarrow d$  emission, consisting of a few relatively sharp bands, is the emission of  $\text{Mn}^{4+}$  in  $\text{Mg}_4\text{GeO}_{5.5}\text{F}:\text{Mn}$  (see Fig. 1.4). Please note that the emitting ion is the same; only its charge (and therefore its electronic configuration) is different. In this case, the optical transition consists of a spin-flip transition within the  $t_{2g}^3$  manifold ( ${}^2\text{E} \rightarrow {}^4\text{A}_2$  transition), i.e. hardly changing the character of the bonding. This manifests itself in relatively narrow emission bands. The spectral structure encountered reflects electron-phonon coupling: the electronic states are coupled to lattice vibrations, which slightly modifies the optical transition energies. This phosphor can be used as red primary in fluorescent lamps. It enables the reproduction of deep red colors. Also in this case, the emission process involves energy transfer. Here, the lattice absorbs the energy, followed by energy transfer to the emitting  $\text{Mn}^{4+}$  ions. This phosphor is one of the few phosphors applied which are sensitized by the host lattice absorption.

The  $d-d$  optical transitions, discussed above, are spin and parity forbidden and consequently rather slow (decay time in the order of ms).

Most rare earth ions show sharp emission bands due to optical transitions within the  $f$ -manifold, e.g.,  $\text{Tb}^{3+}$  ( $4f^8$ -configuration) and  $\text{Eu}^{3+}$  ( $4f^6$ -configuration). See Figs. 1.5 and 1.6 in which the emission spectra of  $(\text{Ce},\text{Tb})\text{MgAl}_{11}\text{O}_{19}$  and  $\text{Y}_2\text{O}_3:\text{Eu}$  are reproduced. Both phosphors are applied in high-quality fluorescent lamps, and  $\text{Y}_2\text{O}_3:\text{Eu}$  is also used in projection television based on cathode ray tubes. In such

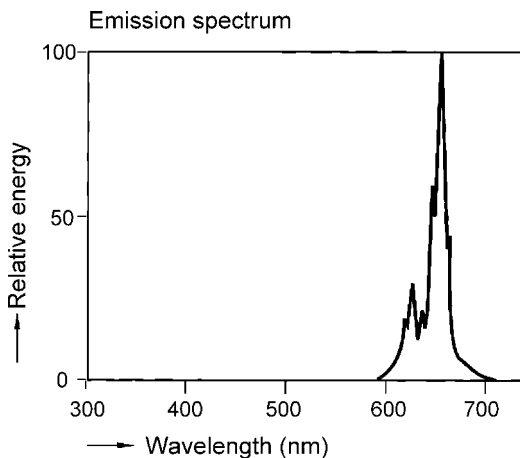


Fig. 1.4  $\text{Mn}^{4+}$  emission in  $\text{Mg}_4\text{GeO}_{5.5}\text{F}$ .

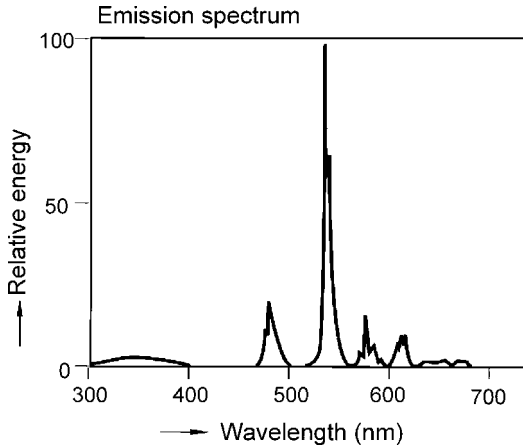


Fig. 1.5 Emission spectrum of  $(\text{Ce,Tb})\text{MgAl}_{11}\text{O}_{19}$ .

projection televisions, small cathode ray tubes are used, the images of which are projected onto a large screen.

There are a few green  $\text{Tb}^{3+}$  based phosphors suitable for application in fluorescent lamps (see Table 1.2).

Especially  $\text{Eu}_2\text{O}_3$  is rather expensive, but despite intensive research, no less expensive substitute for  $\text{Y}_2\text{O}_3:\text{Eu}$  with the same properties has been found, leaving it the only red primary applied with line emission at about 611 nm.

Width and position of the emission bands originating from optical transitions within the f-electronic shell are almost independent of the chemical environment. The relative intensity of the separate bands, however, depends on the crystal lattice. The transitions on many rare-earth ions are spin and parity forbidden and therefore

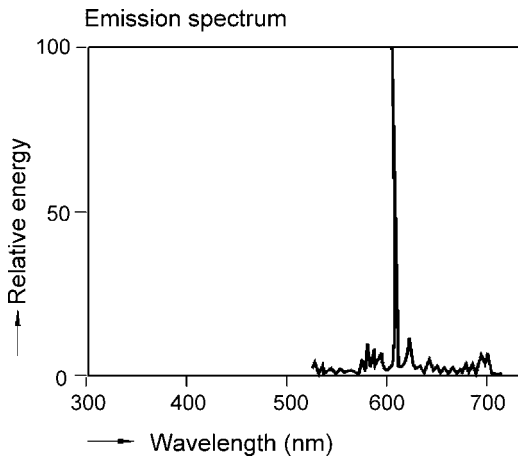


Fig. 1.6 Emission spectrum of  $\text{Y}_2\text{O}_3:\text{Eu}$ .

rather slow (in the ms range). However, for a number of rare-earth ions, broad emission bands are also known, due to  $d \rightarrow f$  emission, e.g.,  $\text{Eu}^{2+}$  ( $4f^7$ -configuration) or  $\text{Ce}^{3+}$  ( $4f^1$ -configuration). These transitions are allowed and consequently very fast (in the  $\mu\text{s}$  range or even faster).

Quite a few very important commercial phosphors are based on rare-earth ions. Rare-earth based phosphors are frequently applied in very demanding applications.

#### 1.4.2

##### Charge Transfer Luminescence

In the case of charge transfer, the optical transition takes place between different kinds of orbitals or between electronic states of different ions. Such an excitation very strongly changes the charge distribution on the optical center, and consequently the chemical bonding also changes considerably. In these cases, therefore, very broad emission spectra are expected.

A very well-known example is  $\text{CaWO}_4$ , used for decades for the detection of X-rays, which shows luminescence originating from the  $(\text{WO}_4)^{2-}$  group (see Fig. 1.7). A similar compound, also showing blue emission, was used in early generations of fluorescent lamps:  $\text{MgWO}_4$ . The transition involves charge transfer from oxygen ions to empty d-levels of the tungsten ion.

In this material no intentional dopant is introduced, and for this reason it is also called self-activated.

#### 1.4.3

##### Donor Acceptor Pair Luminescence

This luminescence mechanism is found in some semi-conducting materials doped with both donors and acceptors. The mechanism is depicted in Fig. 1.8, in which

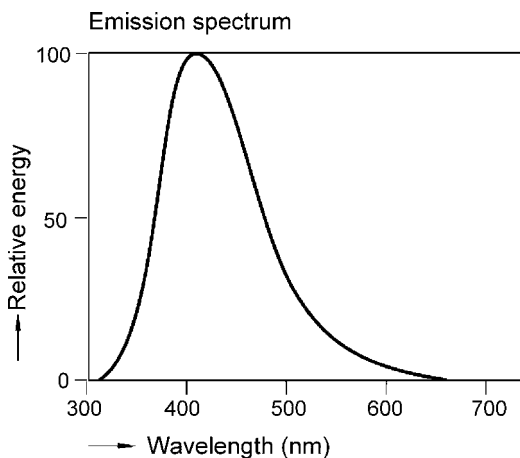


Fig. 1.7 Emission spectrum of  $\text{CaWO}_4$ .

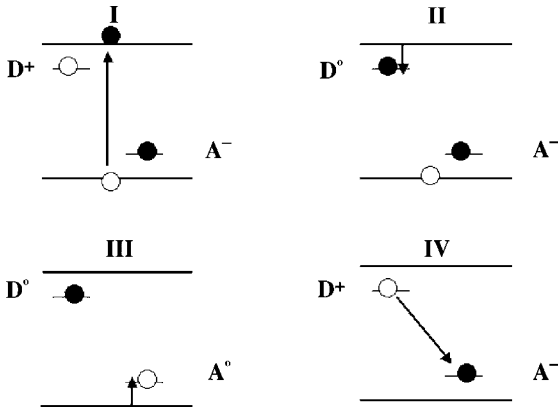


Fig. 1.8 Processes leading to donor-acceptor pair luminescence.

step 4 results in luminescence. Electrons that are excited into the conduction band are captured by ionized donors, and the resulting holes in the valence band are captured by ionized acceptors. The emission involves electron transfer between neutral donors and neutral acceptors. The final state (with ionized donors and acceptors) is Coulomb stabilized. Therefore, the spectral position of the emission generated on a donor-acceptor pair depends on the distance between the donor and the acceptor in a pair: the smaller the distance, the higher the energy of the photon generated.

The energies involved in these processes are:

1. The absorption of energy with the band gap energy, energy involved:

$$-E_g \quad (2)$$

2. Neutralization of the ionized donor, energy involved:

$$E_D - e^2/(4\pi\epsilon_0\epsilon R) \quad (3)$$

in which  $R$  is the distance between donor and acceptor involved in the emission process. The Coulomb term originates from the electrostatic interaction between ionized donor and acceptor.

3. Neutralization of the ionized acceptor, energy involved:

$$E_A \quad (4)$$

4. The luminescence process, energy involved:

$$E_g - (E_A + E_D) + e^2/(4\pi\epsilon_0\epsilon R) \quad (5)$$

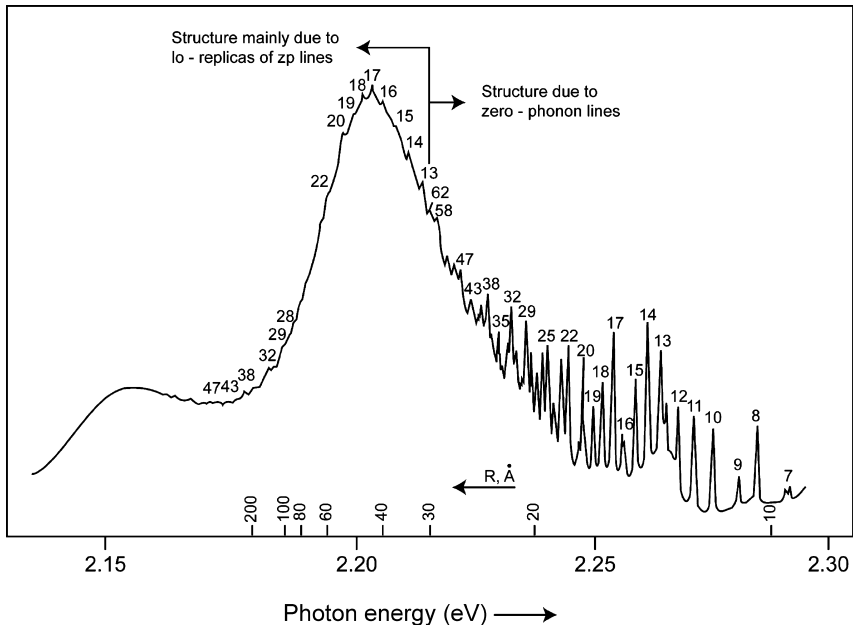


**Fig. 1.9** Donor-acceptor pair luminescence of GaP doped with ZnS.  
From A. T. Vink, thesis, Technical University Eindhoven, 1974.

In the phosphor crystal lattice, many different donor-acceptor distances are possible, but they are restricted by the ionic positions in the lattice. When the interaction of the excited state with the lattice is small, a spectrum with many sharp emission lines occurs. See Fig. 1.9, which shows the emission of GaP doped with ZnS. The numbers in the spectra indicate the donor-acceptor distances (the distance increasing with increasing number associated to the lines). The structure in the right hand part of the spectrum is due to zero-phonon lines, i.e. the emission takes place between the completely relaxed ground and excited state. The structure in the left hand part of the spectrum is due to coupling to host lattice vibrational modes, in this case longitudinal optical phonons.

At larger distances (lower energies), the energy separation between the emission of each of the individual donor-acceptor pairs decreases; as a result, at lower energy a broad emission band is found. The width of the emission band in the case of small interaction with the lattice is given by the Coulomb term. Whether the donor-acceptor mechanism is operative can be deduced easily by a number of techniques:

- Measuring the temporal evolution of the luminescence signal.  
No single exponential decay is expected, as pairs at larger distance will show a smaller radiative recombination rate. For this reason, the decay gets slower as a function of time accompanied by a red shift of the emission spectrum.
- Increasing the excitation density will result in a blue shift of the emission spectrum. This is a consequence of the fact that

emissions at short donor-acceptor pair distances, which have the highest photon energy, have the shortest decay time. The more distant pairs decay much more slowly than the pairs at short distances. Consequently, the more distant pairs saturate, i.e. contribute less to the emission, which rationalizes the blue shift.

This mechanism is operative in the blue and green emitting phosphors, which are used in color television picture tubes (ZnS:Ag,Cl and ZnS:Cu,Au,Al, respectively). In these materials, broad emission bands are found, which are due to a strong electron-phonon coupling of the electronic defect states to vibronic lattice states (see Fig. 1.10).

#### 1.4.4

#### Long Afterglow Phosphors

In long afterglow phosphors, optical excitation energy is stored in the lattice by trapping of photo excited charge carriers. The most prominent example is SrAl<sub>2</sub>O<sub>4</sub>:Eu,Dy: after optical excitation of Eu<sup>2+</sup>, Eu<sup>2+</sup> is oxidized to Eu<sup>3+</sup> and Dy<sup>3+</sup> is reduced to Dy<sup>2+</sup>. Thermal excitation of Dy<sup>2+</sup> to Dy<sup>3+</sup>, followed by capture of the electron by Eu<sup>3+</sup> and subsequent Eu<sup>2+</sup> emission, results in time-delayed Eu<sup>2+</sup> emission. The thermal excitation process of Dy<sup>2+</sup> determines the time delay. This particular material still generates visible emission after several hours in the dark.

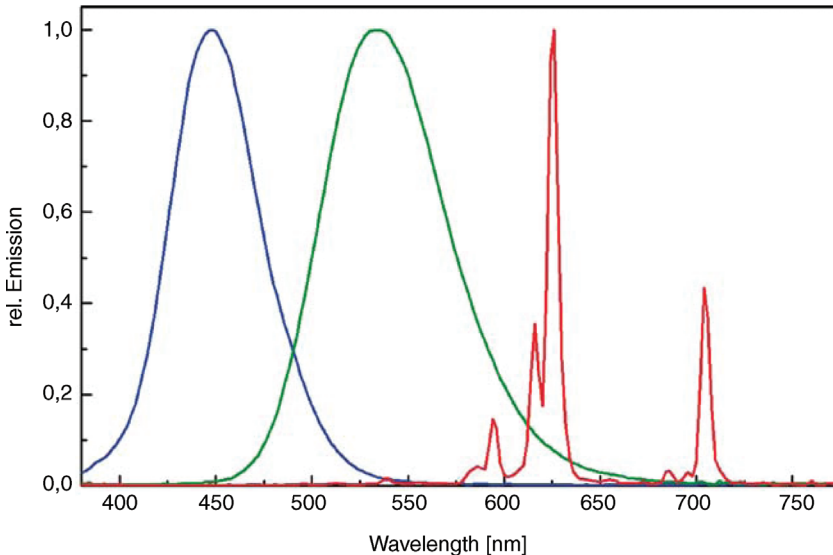


**Fig. 1.10** Emission spectra of ZnS:Ag,Cl (blue-emitting phosphor), ZnS:Cu,Au,Al (green-emitting phosphor), and Y<sub>2</sub>O<sub>2</sub>S:Eu (red-emitting phosphor). The emission of the ZnS phosphors mentioned is of the donor-acceptor pair emission type.

The same mechanism also leads to (undesired) afterglow in scintillating materials, e.g., in  $\text{Gd}_2\text{O}_2\text{S}:\text{Pr,Ce}$ , which is used in Computer Tomography (CT) equipment.

Long afterglow phosphors can be used in watch fingers, but also in safety applications, e.g., in exit signs which still operate in case of a current blackout. Other long afterglow materials are, e.g.,  $\text{ZnS}:\text{Cu}$  and  $\text{SrS}:\text{Bi}$ .

When the energy involved in reversing the trapping process thermally is too high, IR-light absorption might be used to generate visible luminescence. This is the mechanism underlying the use of  $\text{BaFBr}:\text{Eu}$  as X-ray phosphor, as will be discussed in the chapter on scintillators.

## 1.5 Excitation Mechanisms

### 1.5.1 Optical Excitation of Luminescence and Energy Transfer

When absorption of UV or even visible light leads to emission, one speaks of optical excitation of luminescence. This process takes place in, e.g., fluorescent lamps and phosphor-converted LEDs, in which phosphors are used to at least partly change the wavelength of the radiation emitted by the LED. Optical absorption can take place on the already discussed impurities (optical centers), being either the activator ions or the sensitizer ions. Sensitizer ions are used when the optical absorption of the activator ions is too weak (e.g., because the optical transition is forbidden) to be useful in practical devices. In such a case, energy transfer from the sensitizer ions to the activator ions has to take place. The optical absorption leading to emission can also take place by the host lattice itself (band absorption). In this case one speaks of host lattice sensitization. Energy transfer from host lattice states to the activator ions (in some cases also involving sensitizers) has to take place.

In the blue emitting luminescent material  $\text{BaMgAl}_{10}\text{O}_{17}:\text{Eu}$ , both the absorption and the emission processes originate from optical transitions between the 4f and 5d levels of the  $\text{Eu}^{2+}$  ion. As the transition leading to optical absorption is allowed, a relatively small  $\text{Eu}^{2+}$  concentration (10 % of the  $\text{Ba}^{2+}$  ions are replaced by  $\text{Eu}^{2+}$  ions) is sufficient to adjust a sufficiently strong absorption in practical devices. The excitation spectrum of  $\text{BaMgAl}_{10}\text{O}_{17}:\text{Eu}$  is given in Fig. 1.11.

One observes a strong broad absorption spectrum in the UV part of the spectrum as the excited 5d state of the  $\text{Eu}^{2+}$  ion is split by ligand field interaction with the oxygen ions surrounding it. In addition, one observes that the absorption extends into the near UV/blue part of the optical spectrum; this makes this material also suitable for application with near UV LEDs. Phosphors for LEDs are treated in a dedicated chapter in this book.

The excitation spectrum of the  $\text{Mn}^{2+}$  spectrum in  $\text{BaMgAl}_{10}\text{O}_{17}:\text{Eu,Mn}$  is, in the UV, very similar to the excitation spectrum of the compound without  $\text{Mn}^{2+}$ . Here we encounter an example of  $\text{Eu}^{2+}$ -sensitized emission of  $\text{Mn}^{2+}$ , as proven by the similarity of the excitation spectrum of both the  $\text{Eu}^{2+}$  and the  $\text{Mn}^{2+}$  emission. The very localized excitation (exciton) of  $\text{Eu}^{2+}$  is transferred to the  $\text{Mn}^{2+}$  ion. The

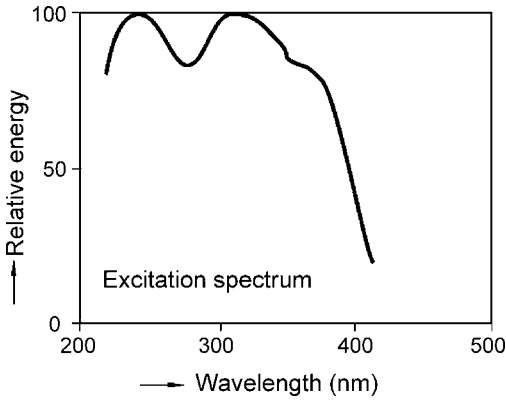


Fig. 1.11 Excitation spectrum of the  $\text{Eu}^{2+}$  emission in  $\text{BaMgAl}_{10}\text{O}_{17}$ .

energy transfer process might involve more than only one  $\text{Eu}^{2+}$  ion. The energy transfer proceeds via the  $\text{Eu}^{2+}$  sub lattice and does not involve charge transport; the underlying mechanism relies on exciton diffusion.

$\text{Mn}^{2+}$  emission can also be sensitized by other ions like  $\text{Sb}^{3+}$  in the well-known white emitting material  $\text{Ca}_5(\text{PO}_4)_3(\text{F},\text{Cl}):\text{Sb},\text{Mn}$ . Here, orange emission is generated by  $\text{Mn}^{2+}$  and blue emission by the  $\text{Sb}^{3+}$ . This material is applied widely in fluorescent lamps. The emission of this material is perceived as white. Its emission spectrum is given in Fig. 1.12.

Please note that the emission spectrum depends on the  $\text{Sb}^{3+}$  and  $\text{Mn}^{2+}$  concentrations. By adjusting these concentrations, the color temperature of the emission can be varied.

Another well-known sensitizer-activator pair is the  $\text{Ce}^{3+} - \text{Tb}^{3+}$  couple (see Fig. 1.5 and Table 1.4 below). All green emitting phosphors applied in high-quality fluorescent lamps are based on this combination.

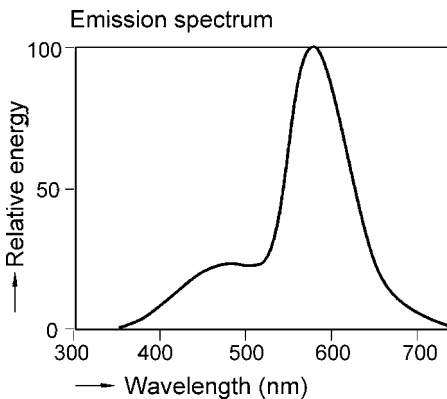


Fig. 1.12 Emission spectrum of  $\text{Ca}_5(\text{PO}_4)_3(\text{F},\text{Cl}):\text{Sb},\text{Mn}$ .

## 1.6 Energy Transfer Mechanisms Between Optical Centers

Energy transfer between a sensitizer ion (S) and an activator ion (A) can be written as a chemical reaction:



where the asterisk indicates the excited state.

We remark that sensitization can involve even more ions, as in (Ce,Gd,Tb)Mg-B<sub>5</sub>O<sub>10</sub>:Mn (a green and red emitting luminescent material applied in fluorescent lamps with a very high color rendering), where the energy is transferred from the Ce<sup>3+</sup> ions to the Tb<sup>3+</sup> and the Mn<sup>2+</sup> ions via the Gd<sup>3+</sup> ion sub lattice. The emission spectrum is given in Fig. 1.13. We observe green Tb<sup>3+</sup> emission, red Mn<sup>2+</sup> emission, and a trace of Ce<sup>3+</sup> emission in the UV, indicating that the energy transfer efficiency is almost completely unity.

### 1.6.1 Mechanisms Underlying Energy Transfer

For energy transfer, the sensitizer ion and the activator ion have to show physical interaction. This energy transfer can find its origin in electrostatic and exchange interaction. In addition, the emission spectrum of the sensitizer ion and the absorption spectrum of the activator ion have to show spectral overlap, for energy conservation reasons.

The probability  $W_{et}$  for energy transfer is given by the following term:

$$W_{et} = 2\pi/\hbar(\rho)[\varphi_i|H|\varphi_f]^2 \quad (7)$$

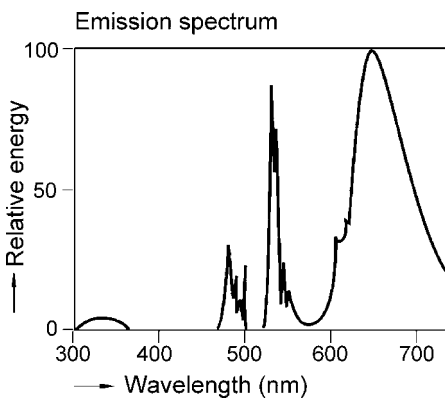


Fig. 1.13 Emission spectrum of (Ce,Gd,Tb)(Mg,Mn) B<sub>5</sub>O<sub>10</sub>.

In this term,  $\varphi_i$  is the wave function of the initial state,  $\varphi_f$  is the wave function of the final state,  $\rho$  is a measure for the density of initial and final states capable of interaction, and  $H$  is the operator coupling the initial and final state.  $\rho$  is given by

$$\rho = \int g_s(E)g_A(E)dE \quad (8)$$

representing the spectral overlap between sensitizer and activator ions.  $g_s(E)$  and  $g_A(E)$  are the normalized optical line shape functions for the sensitizer and the activator ions, respectively.

In this treatment we distinguish between two kinds of interactions: electrostatic interaction given by  $H_c$  and exchange interaction described by  $H_e$ . The probability per unit time for energy transfer then can be written as

$$W_{et} = 2\pi/\hbar(\rho)\{[\varphi(S^*)\varphi(A)|H_c|\varphi(S)\varphi(A^*)]^2 + [\varphi(S^*)\varphi(A)|H_e|\varphi(S)\varphi(A^*)]^2\} \quad (9)$$

The matrix elements for Coulomb interaction represent the repulsive electrostatic interaction between the electronic charge distributions in the initial and final state, respectively, and have the following shape:

$$Q_i^C = \varphi_{s^*}(1)\varphi_A(2) \text{ and } Q_f^C = \varphi_s(1)\varphi_{A^*}(2) \quad (10)$$

The matrix elements for exchange interaction represent the repulsive electronic interaction of the electronic charge distributions, and have the following shape:

$$Q_i^e = \varphi_{s^*}(1)\varphi_A(2) \text{ and } Q_f^e = \varphi_s(2)\varphi_{A^*}(1) \quad (11)$$

In Fig. 1.14, electronic energy transfer by Coulomb and exchange interaction are compared. In the case of Coulomb interaction, the electrons initially on the excited donor stay there, and the electrons initially on the acceptor also remain there. This interaction does not require physical contact between the interacting partners; it is sufficient that the excited sensitizer ion induces a dipole oscillation on the activator ion. In the case of energy transfer governed by exchange interaction, the way the energy is transferred can be visualized by a double electron substitution reaction: the excited electron on  $S^*$  travels to A, whereas one electron on A goes to S. This type of interaction requires overlap of the electronic charge distribution, i.e. physical contact between the sensitizer ion and the activator ion.

### 1.6.2

#### Energy Transfer Governed by Electrostatic Interaction

In this section, we discuss, using a simple model, the factors governing the magnitude of the electrostatic interaction and how they relate to the rate of energy transfer.

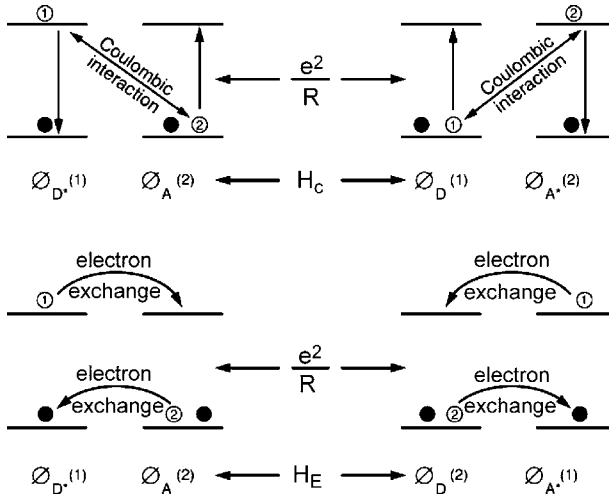


**Fig. 1.14** Visualization of energy transfer by Coulomb interaction (a) and exchange interaction (b) between two ions.

The interaction energy  $E_{SA}$  between two dipoles is given by the magnitude of the two dipoles ( $\mu_S$  and  $\mu_A$ , respectively) and the distance  $R_{SA}$  between them:

$$E_{SA} \propto \mu_S \mu_A / R_{SA}^3 \quad (12)$$

Förster [1–3] has identified  $\mu_S$  and  $\mu_A$ , respectively, with the oscillator strength for the radiative transitions  $S^* \leftrightarrow S$  and  $A^* \leftrightarrow A$ , respectively. We will now treat energy transfer more quantitatively.

The power irradiated by an oscillating dipole  $\mu \cos \omega t$  is given by

$$P = 4\omega |\mu|^2 / 3c^3 \quad (13)$$

The result obtained is a factor of 4 larger than in classical electrodynamics, to differentiate between photons absorbed and emitted.

The rate of decay  $A$  is given by Eq. (14) (energy emitted per unit time divided by the photon energy  $\hbar\omega$ ):

$$A = 1/\tau_0 = (4\omega |\mu|^2 / (3c^3)) / (\hbar\omega) \quad (14)$$

in which  $\tau_0$  is the radiative lifetime.

We obtain for  $|\mu|^2$ :

$$|\mu|^2 = 3hc^3 / (8\pi\omega^3 \tau_0) \quad (15)$$

The oscillator strength for an optical transition is related to  $|\mu|^2$  in the following way:

$$f = 2m\omega|\mu|^2/(3\hbar e^2) \quad (16)$$

$|\mu|^2$  is thus given by

$$|\mu|^2 = (3\hbar e^2)f/(2m\omega) \quad (17)$$

Apart from some numbers we are now able to calculate the rate of energy transfer from sensitizer ions to activator ions, being the product of equation (14) for the sensitizer and (17) for the activator ion divided by the distance  $R_{SA}^6$  (see above, the transition rate contains the matrix element for the energy squared):

$$W_{SA} \propto 3\hbar c^3/(8\pi\omega^3\tau_{0S})(3\hbar e^2)f_A/(2m\omega R_{SA}^6) \quad (18)$$

Or, after some rearrangements and inclusion of the numbers mentioned above (which partly originate from the expansion of the interaction Hamiltonian in spherical harmonics), the following equation is obtained [4]:

$$W_{SA} = 2\pi/\hbar/R_{SA}^6 \cdot 3e^2c^3\hbar^6/4m \cdot f_A/\tau_S \cdot \eta \cdot \int g_S(E)g_A(E)/E^4 dE \quad (19)$$

In this equation,  $\tau_S$  is the decay time of the sensitizer ion and  $\eta$  is the quantum efficiency of the sensitizer ion.

Equation (19) can also be written as:

$$W_{SA} = 1/\tau_S \cdot (R_0/R_{SA})^6 \quad (20)$$

where  $R_0$  is the distance at which the transfer rate to the activator is equal to the decay rate of the sensitizer and is given by:

$$R_0^6 = \eta f_A (3e^2c^3\hbar^5\pi/2m) \int g_S(E)g_A(E)/E^4 \cdot dE \quad (21)$$

Inspection of the equations derived shows that energy transfer, governed by Coulomb interaction, is favored by a large spectral overlap, a small value of the intrinsic decay time of the sensitizer ion, a large absorption strength of the activator ion, and a small distance between the sensitizer and activator ion.

In practice, it is of more importance to determine the efficiency of the energy transfer process than the rate.

The decay of the sensitizer ion is given by:

$$1/\tau_S = 1/\tau_0 + 1/\tau_S \cdot R_0^6/R_{SA}^6 \quad (22)$$

The yield  $\eta_{SA}$  for energy transfer is therefore given by:

$$\eta_{SA} = 1/\tau_S \cdot R_0^6/R_{SA}^6/(1/\tau_S) \quad (23)$$

the energy transferred per unit time divided by the total amount of energy emitted per unit time.

For the efficiency of the energy transfer process  $\eta_{SA}$ , we therefore find the following proportionality:

$$\eta_{SA} = (R_0/R_{SA})^6 \quad (24)$$

Please note that the quantum efficiency of the sensitizer ion is contained in  $R_0$  [see Eq. (21)]. For a distance  $R_{SA}$  between the sensitizer ion and the activator ion smaller than  $R_0$ , energy transfer will dominate; in the opposite case, inherent decay of the sensitising ion  $S^*$  is the most important process. Moreover, though the energy transfer rate increases with decreasing  $\tau_S$ , the same applies to the sensitizer emission probability. Therefore, the transfer yield is independent of  $\tau_S$ .

### 1.6.3

#### Energy Transfer by Higher-order Coulomb Interaction

Apart from dipolar interaction, higher-order interaction may also result in energy transfer. In Table 1.1, the distance dependence of interaction involving dipoles and quadrupoles is summarized for the case that the optical transitions involved are spin allowed:

A more quantitative analysis, using the expressions derived above, shows that in the case of electric dipole interaction:

- Energy transfer from a broad-band emitter to a line absorber only occurs between nearest neighbors.
- Energy transfer from a line emitter to a broad-band absorber is possible for distances up to about 2 nm.
- Energy transfer from a broad-band emitter to a broad-band absorber is possible for distances as large as about 3.5 nm.
- Dipole-dipole interactions and dipole-quadrupole interactions can result in energy transfer in solids: both interactions can take place over metal ion–metal ion distances which are observed in solids.
- Interactions between electric quadrupoles are not expected to play an important role in solids in view of the very short interaction range.

**Tab. 1.1** Equations for energy transfer governed by Coulomb interaction as a function of the type of interaction for spin-allowed transitions.

Interaction type	Equation form	Range (nm)
Electric dipole – electric dipole	$W_{SA} = (1/\tau_S) (R_0/R_{SA})^6$	3.5
Electric dipole – electric quadrupole	$W_{SA} = (1/\tau_S) (R_0/R_{SA})^8$	0.8
Electric quadrupole – electric quadrupole	$W_{SA} = (1/\tau_S) (R_0/R_{SA})^{10}$	0.2

## 1.6.4

**Energy Transfer Governed by Exchange Interactions**

Dexter has formulated a theory describing energy transfer by exchange interaction [5]. The rate constant for energy transfer is written as

$$W_{SA} = KJ \exp(-2R_{SA}/L) \quad (25)$$

In equation (25),  $K$  is a constant determined by the interaction between the orbitals involved in the energy transfer process,  $J$  is determined by the spectral overlap integral, normalized for the absorption strength of the activator ion, and  $L$  is determined by the van der Waals radii of the interacting ions. The exponential dependence is due to the fact that the electron density in general falls off exponentially with the distance between the electron and the nucleus.

As the energy transfer process does not involve electric dipole interaction, no dependence of the magnitude of the electric dipoles on the sensitizer and activator ions is expected. In view of the relationship between the magnitude of the electric dipoles and the oscillator strength (see above), therefore, no relation between the oscillator strength of the optical transitions on sensitizer and activator ion is expected. In fact, for exchange interaction, there is no relation between the interaction between the ions and any spectroscopic characteristic of the sensitizer or activator ions.

Another difference between energy transfer governed by Coulomb and exchange interaction is the distance dependence. The rate of energy transfer shows an  $R_{SA}^{-n}$  dependence in the case of Coulomb interaction and an  $\exp(-R_{SA}/L)$  dependence in the case of energy transfer by exchange interaction. In the case of energy transfer by exchange interaction, the rate drops very quickly for distances  $R_{SA}$  greater than about 1 nm.

Finally, exchange interaction, due to the requirement of wave function overlap, has a pronounced angular dependency and is also dependent on covalence.

## 1.6.5

**Cross-relaxation and Energy Transfer**

A phenomenon not discussed until now is cross-relaxation. In such a process, which can also be looked upon as energy transfer, the excited ion transfers only part of its energy to another ion. For two  $Tb^{3+}$  ions, the process is depicted in Fig. 1.15. In this case, the energy difference between the  $^5D_3$  and  $^5D_4$  excited states matches approximately the energy difference between the  $^7F_6$  ground state and higher  $^7F_j$  states. As in the energy transfer processes discussed above, at large Tb-Tb distances, the process of cross-relaxation has a low rate. In many host lattices, therefore, at low Tb concentration, emission from both the  $^5D_3$  and  $^5D_4$  excited states is observed (unless the gap between these two states is bridged by phonon emission, for which relatively high-energy phonons are required, which is, for example, the case with  $InBO_3:Tb$ ). The resulting emission spectrum has emission from the near UV into the red part of

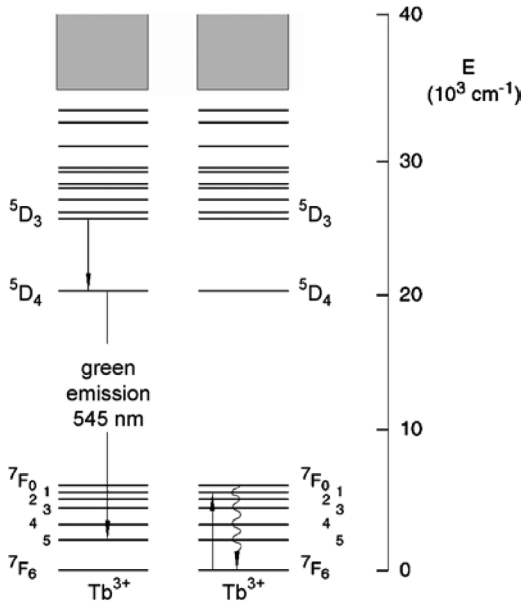


Fig. 1.15 Cross-relaxation between two  $\text{Tb}^{3+}$  ions.

the optical spectrum. At higher Tb concentrations (in the order of five percent), cross-relaxation quenches the emission from the  ${}^5\text{D}_3$  level in favor of emission originating from the  ${}^5\text{D}_4$  level, implying that it is not possible to obtain blue  $\text{Tb}^{3+}$  emission in luminescent materials with higher  $\text{Tb}^{3+}$  concentrations.

Cross-relaxation also occurs for other ions. It quenches blue  $\text{Eu}^{3+}$  emission even at relatively low  $\text{Eu}^{3+}$  concentrations (<1%) in favor of the well-known red emission. In case of ions like  $\text{Sm}^{3+}$  and  $\text{Dy}^{3+}$ , cross-relaxation leads to quenching of the visible emission. This seriously limits the applicability of these ions.

### 1.6.6

#### Practical Implications

Of course, the arguments developed above have practical implications. In general, the activator ions used in luminescent materials are rather expensive. This implies that the concentration of the activator ions should be as low as possible. When energy transfer processes are important, the smallest activator concentrations are possible for the case of broadband-emitting sensitizers and broadband-absorbing activators. On the other hand, for high-quality fluorescent lamps, line emitters are required to obtain an optimized adaptation of the emission spectrum to the human eye with respect to the amount of visible light generated and the need to reproduce all colors in a natural way. As discussed above, this requires that sensitizer ion and activator ion are nearest neighbors, i.e. at least one of the two kinds of ions should be present in relatively high concentrations.

When optical absorption on the activator ions is forbidden at the energy where the sensitizer ion emits (the activator ions, however, should have an excited state there), in principle there are nevertheless two options to obtain energy transfer:

- Coulomb interaction exploiting the quadrupole of the activator ion. This is the mechanism underlying the fluorescent lamp phosphors  $\text{BaMgAl}_{10}\text{O}_{17}:\text{Eu},\text{Mn}$  [6] and  $(\text{Ce},\text{Tb})\text{MgAl}_{11}\text{O}_{19}$  [7]. Because of the vanishingly small spectral overlap between the  $\text{Ce}^{3+}$  absorption and the emission bands, no energy migration between the Ce ions takes place. This requires not only short Ce-Tb distances in this luminescent material, but also relatively high Tb concentrations, to prevent Ce emission from occurring.
- Exchange interaction between sensitizer and activator ion. As shown above, this mechanism does not require allowed optical transitions. This is the mechanism which is operative in the one-component white fluorescent lamp phosphor  $\text{Ca}_5(\text{PO}_4)_3(\text{F},\text{Cl}):\text{Sb},\text{Mn}$ , as deduced from an analysis of the decay curve for some  $\text{Mn}^{2+}$  concentrations [8]. The same study did not reveal evidence for energy transfer between antimony ions, indicating the necessity of nearest neighbor Sb-Mn interaction, which is a prerequisite for energy transfer via exchange interaction. Please note, in addition, that in view of the large Stokes shift between absorption and emission on the  $\text{Sb}^{3+}$  ion in this lattice, no energy transfer between the antimony ions is expected.

Both for electric dipole – electric quadrupole and exchange interaction, the distance between sensitizer ion and activator ion has to be rather small, not larger than about 1 nm. This requires high activator and/or sensitizer ion concentrations, which is a disadvantage, considering the high costs of these materials.

## 1.7

### Excitation with High-energy Particles

After absorption of electrons or high-energy photons (e.g., X-ray quanta) impinging on the phosphor material, primary electrons and holes in very deep shells are created. Whereas the holes are tightly bound, the electrons can move in the lattice (and a fraction of the electrons generated can leave the material). The primary ionization event is followed by radiative decay (secondary X-rays, the basis for EDAX), non-radiative decay (the generation of secondary electrons by Auger processes), and inelastic electron-electron scattering. These processes are very fast and occur typically in the  $10^{-15}$ – $10^{-13}$  s regime after the primary absorption. During these processes, many electrons are excited.

When the energy of the electrons generated is lower than the ionization threshold, the hot electrons and holes thermalize by intraband transitions and electron-optical

phonon interaction. Also during this process, activator or sensitizer ions may be excited by impact excitation by hot electrons, by sequential excitation by capture of mobile charge carriers (electrons and holes), and by excitons. These processes typically occur in a time frame  $10^{-12}$ – $10^{-8}$  s and may therefore lead to a clearly visible rise time of the emission.

In the last step, luminescence can occur in a time frame of  $10^{-9}$  s for very fast allowed optical transitions up to ms or even longer times for forbidden transitions.

Robbins has treated these processes more quantitatively [9]. In this chapter, we only outline this excellent treatment. The more interested reader is referred to the original paper.

The energy efficiency of the overall process is given by

$$\eta = (1 - r)[h\nu]/(\beta E_g) \cdot \eta_t \eta_{act} \eta_{esc} \quad (26)$$

in which  $r$  is the backscatter coefficient, expressing the fact that not all high-energy particles enter the material,  $[h\nu]$  is the mean photon energy of the photons emitted,  $\beta E_g$  the energy needed to generate a thermalized electron-hole pair ( $\beta$  being a pure number and  $E_g$  being the band gap energy),  $\eta_t$  is the transfer efficiency of electron-hole pairs to activators or sensitizers,  $\eta_{act}$  is the quantum efficiency of the activator ions (which gives the ratio of the number of photons emitted divided by the number of photons absorbed), and finally  $\eta_{esc}$  is the ratio between photons leaving the material and photons generated in the material (escape probability).

Backscattering is negligible for X-rays, whereas for electrons the backscatter coefficient  $r$  generally has values between 0.1 and 0.2.

For applications, phosphors operating at physical limits are of interest only. This means that the transfer efficiency, the activator efficiency, and the escape probability have to be unity. Equation (26) then simplifies to

$$\eta = (1 - r)[h\nu]/\beta E_g \quad (27)$$

Inspection of this equation shows that the energy efficiency is determined by the mean energy of the photons emitted by the activator ions and by the product  $\beta E_g$ . The primary particles, eventually generating the luminescence, lose their energy by impact ionization and generation of optical phonons. In what follows, we discuss this mechanism in some more detail. It is important to note that the description boils down to calculating what fraction of the energy that impinges on the material is used to create electron-hole pairs with energy (almost) equal to the band gap energy. The energy might be slightly smaller than the band gap energy, as the electron and the hole can attract each other by Coulomb interaction. In such a case an exciton is formed. Further, the reader should carefully note that this treatment gives the maximum efficiencies only.

In Chapter 5, which deals with scintillating materials, we will use expression (27) in a slightly different form. In scintillator physics, the light yield is generally expressed in the units [photons/MeV of excitation energy]. Scintillating materials can generate more than 70 000 photons per MeV of excitation energy. For scintillators, the light

yield is more useful than the energy efficiency in view of the fact that photons are to be detected.

The average energy needed to create an electron-hole pair can be written as

$$\beta E_g = E_i + E_{op} + 2E_f \quad (28)$$

In this expression,  $E_i$  is the ionization threshold,  $E_{op}$  the average energy lost in generating optical phonons, and  $E_f$  is the threshold energy for the generation of electron-hole pairs.

The ratio of the energy needed to generate optical phonons with frequency  $\hbar\omega_{LO}$  and impact ionization is proportional to  $R$ , which in turn is given by

$$R = (1/\varepsilon_\infty - 1/\varepsilon_0)(\hbar\omega_{LO})^{1.5}/(1.5 E_g) \quad (29)$$

in which  $\varepsilon_\infty$  and  $\varepsilon_0$  are the optical and static dielectric constants of the phosphor host lattice, respectively. The dependence of  $\beta$  on  $R$  is given in Fig. 1.16, in which a slightly different notation for the expression dealing with the dielectric constants is used.

The value of  $\beta$  is found to vary between about 2.5 and 10 for a number of host lattices. We observe that in order to obtain host lattices with small  $\beta$ , resulting in highly efficient phosphors, the value of  $R$  should be small as well. This condition implies a low optical phonon frequency or a small difference between the optical and the static dielectric constant. In Table 1.2, the relevant data are given for a number of well-known phosphor materials. We observe a good agreement between the energy efficiencies observed and the maximum efficiencies predicted.

Please note that this treatment deals with host lattice properties only, i.e. it is the host lattice properties which decide whether the impinging energy is efficiently converted into energy gap excitations. This is in line with observations: quite a few host lattices show efficient cathode rays from X-ray excited luminescence when doped with different activators. Examples are ZnS, CaS (see Table 1.2) and the rare

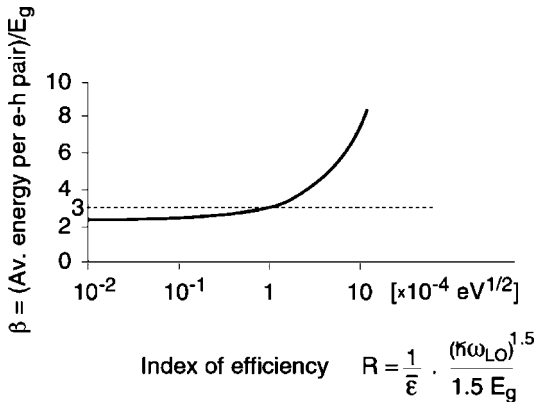


Fig. 1.16 Dependence of  $\beta$  on  $R$ .

**Tab. 1.2** Physical constants of a number of efficient host lattice-excited phosphors.  $\eta_{\text{the}}$  is the maximum efficiency calculated,  $\eta_{\text{exp}}$  is the energy efficiency observed experimentally.

Phosphor	$\hbar\omega_{\text{LO}}$ (eV)	$E_g$ (eV)	$[\hbar\nu]$ (eV)	$\beta$	$\eta_{\text{the}}$	$\eta_{\text{exp}}$
CsI:Tl	0.011	6.4	2.25	2.5	0.14	0.14
ZnS:Ag	0.044	3.8	2.75	2.9	0.25	0.20
ZnS:Cu	0.044	3.8	2.3	2.9	0.21	0.17
CaS:Ce	0.047	4.8	2.3	3.0	0.16	0.22
CaS:Mn	0.047	4.8	2.1	3.0	0.15	0.16
La <sub>2</sub> O <sub>2</sub> S:Eu	0.057	4.4	2.0	3.9	0.12	0.11
Y <sub>2</sub> O <sub>3</sub> :Eu	0.068	5.6	2.0	4.6	0.07	0.08
YVO <sub>4</sub> :Eu	0.116	3.7	2.0	7.5	0.07	0.07

earth oxysulfides (like Gd<sub>2</sub>O<sub>2</sub>S, which shows efficient emission when doped with Pr<sup>3+</sup>, Eu<sup>3+</sup> or Tb<sup>3+</sup>).

The mechanism discussed above involves efficient energy transfer from host lattice states to localized states. This mechanism also occurs in some luminescent materials applied in Xe-discharges. The Xe-discharge generates radiation in the VUV part of the spectrum. In these materials, the host lattice itself acts as sensitizer.

We remark that an alternative description for the generation of electron-hole pair generation has been formulated [10]. In this model,  $\beta$  can be much smaller than the values derived by Robbins (close to unity and virtually material independent). In this model, transfer from host to activator ions is the energy efficiency determining step. Interesting feature of this model is that also ionic materials could have very high photon yields.

## 1.8 Electroluminescence (EL)

### 1.8.1 High-voltage Electroluminescence

High-voltage electroluminescence relies on an electrical breakthrough in a semi-conducting material, which rationalizes the necessity to use rather high voltages. Generally speaking, the lifetime of such electroluminescent devices can be long but the efficiencies are rather low (in the order of one percent, see below) and consequently applications are found in segments where reliability is an issue and efficiency considerations are not very important (emergency signs, exit signs, and interestingly ceiling illumination in the Maybach premium car). Prominent materials are ZnS:Mn, ZnS:Cu, and SrS:Ce, although oxides are under investigation as well.

The luminescent materials are used in thin layers (in the order of 1  $\mu\text{m}$ ) generated by techniques like atomic- or molecular beam epitaxy, although powder EL is also known. The materials are subjected to high electric fields, and electrons are accelerated in the materials. The electrons excite the activator ions by impact excitation. At present, there is no general picture of the mechanism(s) underlying high-voltage electroluminescence.

We will give a very elementary treatment, which yields the energy efficiency to be expected, without considering the mechanism(s) in detail.

The maximum efficiency  $\eta$  is given by:

$$\eta = E_{em}\sigma N/eF \quad (30)$$

in which  $E_{em}$  is the photon energy of the emitted radiation,  $\sigma$  the cross-section for impact excitation,  $N$  the optimum concentration of luminescent centers, and  $F$  the electric field applied. Dimensional analysis shows that  $(\sigma N)^{-1}$  has the units [m]. The physical meaning of  $(\sigma N)^{-1}$  is the mean distance that an electron travels through the luminescent material between two excitation events.

The cross-section is not known *a priori*. In the case of ZnS:Mn (the most efficient ACTFEL material known), we approximate it by using atomic dimensions, i.e.  $\sigma = 10^{-16} \text{ cm}^2$  (the  $\text{Mn}^{2+}$  ions has the same charge and approximately the same size as the  $\text{Zn}^{2+}$  ion). The other typical values are:  $E_{em} = 2 \text{ eV}$ ,  $N = 10^{20} \text{ cm}^{-3}$  and  $F = 10^6 \text{ V cm}^{-1}$ . It follows that the energy efficiency equals about 2 %, which is in very good agreement with experiment. In this treatment, however, we have used a number of simplifications. We did not account for the Stokes shift. Moreover, we neglected light-trapping effects in the thin layers. All these phenomena further reduce the energy efficiency. However, the energy efficiency is not likely to be improved significantly. This is mainly because of the low value for the cross-section, because  $N$  cannot be chosen to be too large in view of concentration quenching.

The mean energy that the charge carrier has taken up from the electric field between two impact excitation events equals  $eF/\sigma N$ , neglecting any losses due to phonon emission. The minimum pathway that an electron has to travel to be able to excite an activator ion  $L_{crit}$  equals  $L_{crit} = E_{exc}/eF$ , where  $E_{exc}$  is the energy needed for the excitation of the luminescence. Please note that  $L_{crit}$  is dependent on the electric field strength. Incorporation of  $L_{crit}$  in Eq. (30) yields

$$\eta = E_{em}/E_{exc} \cdot \sigma N \cdot L_{crit} \quad (31)$$

In the case of excitation of luminescence via host-lattice states (see above), the luminescence efficiency can be written very generally as

$$\eta = E_{em}/E_{exc} \cdot \eta_t \cdot \eta_{act} \cdot \eta_{esc} \quad (32)$$

In this expression  $\eta_t$  is the probability of energy transfer from the host lattice to the activator ions,  $\eta_{act}$  is the quantum efficiency of the activator, and finally  $\eta_{esc}$  is the escape probability – the ratio between the number of photons leaving the material and the number of photons generated in the material. On assuming  $\eta_{act}$  and  $\eta_{esc}$  to be unity, the maximum energy efficiency for the ACTFEL process is given by:

$$\eta = E_{em}/E_{exc} \cdot \eta_t \quad (33)$$

Inspection of Eqs. (31) and (33) leads to the conclusion that  $\sigma N \cdot L_{crit}$  is the transfer efficiency. In case of cathode ray excitation, this figure can be unity. In case of

ZnS:Mn, its optimal value is calculated to be about 0.02 only. The low transfer efficiency of energy from host lattice states to activator states is the main reason for the low energy efficiency of this material, but still it is the most efficient one known! Please note that this equation shows that the maximum efficiency of EL phosphors is determined by both host-lattice and dopant properties.

### 1.8.2

#### Low-voltage Electroluminescence

The advent of the blue light-emitting diode (LED) and of organic electroluminescent structures has strongly revitalized interest in this luminescence mechanism. For the first time, efficient light-emitting structures can be realized which do not require either high or low pressure. In addition, luminescent devices have always hitherto used a cascade – in fluorescent lamps, first a discharge is generated and the resulting invisible radiation is converted into visible light, resulting in a (considerable) energy loss. In cathode ray tubes, first an electron beam consisting of electrons with rather high kinetic energy is generated, which subsequently impinges on the luminescent material. In the phosphors, electron bombardment finally leads to excitations where electrons in the conduction band are coupled to holes in the valence band (excitons). These excitons are transferred to activator ions. As a result, there are no white light-emitting devices with energy efficiency greater than 50 %. Low-voltage electroluminescent devices might be a way out here. In such devices, the step leading to emission is the recombination of electrons in conduction band states with holes in valence band states, and in principle only the band gap energy is required to excite the luminescence. Within limits, the color of the emission can be selected by choosing the appropriate semiconductor. The generation of luminescence can be very energy efficient; the main issue is getting the light out of the emitting device. LEDs are available with wall plug efficiency approaching 70 %.

Apart from efficiency, the power dissipated by LEDs is also an important driver, as it contributes to the light output that such a device can generate. Lighting applications generally require a light output of 1 W and above. LEDs with input power of 30 W and external energy efficiency of about 10 % have been demonstrated by the Japanese company Nichia and Philips Lumileds.

In this book, luminescent materials that can be used in inorganic low-voltage electroluminescent devices are discussed in a separate chapter. Phosphors are used for two reasons:

- Inorganic LEDs generally generate narrow line emission. Combination of LEDs emitting in different spectra regions to generate white light therefore results in white light of low quality: it cannot reproduce all colors in a natural way.
- Efficient LEDs are not yet available in all colors required. Especially green is a concern.

Phosphors for LEDs have to fulfill rather harsh conditions. The Stokes shift must be small, the absorption must be high, and, in addition, as the excitation densities are

in the order of  $20 \text{ W cm}^{-2}$  (the area which emits light is much smaller than, e.g., in fluorescent lamps), the luminescent materials must remain efficient up to high temperatures, should not show saturation (meaning a less than linear increase in output power with input power at high excitation densities), and must be radiation stable.

## 1.9 Factors Determining the Emission Color

Many luminescent ions show emission at different wavelengths in different host lattices. This phenomenon, once understood, opens up the possibility to change, within certain limits, the emission color. In this way, the emission spectra (and excitation spectra) can be tuned toward the specifications required.

In cases where at least one of the electronic states is involved in the chemical bonding, the coupling to the lattice has to be taken into account. This situation is encountered for many transition metal ions, for the  $s^2$  ions, and for rare-earth ions showing  $d \rightarrow f$  emission.

In Fig. 1.17, this situation is illustrated for  $d \rightarrow f$  optical transition on  $\text{Eu}^{2+}$ .

Other rare-earth ions showing  $d \rightarrow f$  emission are  $\text{Ce}^{3+}$ ,  $\text{Pr}^{3+}$ ,  $\text{Nd}^{3+}$  and  $\text{Er}^{3+}$ , albeit for the last three ions only in the UV.

The energy difference between the d- and f-electrons is modified by the covalence of the  $\text{Eu}^{2+}$ -ligand bond and the crystal field strength. An increase of the covalence of the  $\text{Eu}^{2+}$ -ligand bond results in a lower energy difference of the 4f-5d energy separation (due to the nephelauxetic effect). This elementary treatment considers the shift of the center of gravity (also called barycenter) of the d-electron level (also called centroid shift), i.e. any splitting is not yet taken into account. The crystal field

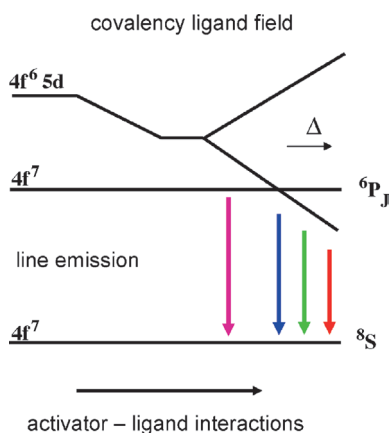


**Fig. 1.17** Energy separation of the  $4f^7$  and  $4f^6 5d^1$  bands as a function of covalence and ligand field strength. The arrows indicate different emission colors.

**Tab. 1.3** Spectral position of the emission band of  $\text{Eu}^{2+}$  in some representative lattices.

$\text{SrB}_4\text{O}_7:\text{Eu}$	368 nm
$\text{Sr}_2\text{P}_2\text{O}_7:\text{Eu}$	420 nm
$\text{BaMgAl}_{10}\text{O}_{17}:\text{Eu}$	453 nm
$\text{Sr}_4\text{Al}_{14}\text{O}_{25}:\text{Eu}$	490 nm
$\text{Ba}_2\text{SiO}_4:\text{Eu}$	505 nm
$\text{SrGa}_2\text{S}_4:\text{Eu}$	535 nm
$\text{Sr}_2\text{SiO}_4:\text{Eu}$	575 nm
$\text{SrS}:\text{Eu}$	615 nm

interaction splits the d-level, depending on symmetry and crystal field strength. In this way, e.g., for  $\text{Eu}^{2+}$ , emission can be obtained extending from the UV part of the optical spectrum (where even line emission is possible [11]) to the red part (see Table 1.3). Both are easily accessible by choosing appropriate host lattices, and for this reason broad-band emitters can in general be tuned within a large spectral range and can be adapted to the application needs.

The spectral position of the emission lines due to transitions between f-electronic states does not vary very much on changing the host lattice. However, the relative emission intensity of the several possible optical transitions does vary considerably.

As general remark, one can state that in cases where the rare-earth ion occupies a site with inversion symmetry, the selection rule states:  $\Delta J = 0, 1$ . In cases where  $\Delta J = 0$ , any transition to another state with  $J = 0$  is forbidden as well. In such a case,  $\Delta|J|$  is necessarily  $+1$ . These are all magnetic dipole transitions. In lattices without inversion symmetry there is also electric dipole emission. For these transitions, the selection rule is:  $\Delta|J| \leq 6$ . Here again, for initial or final states with  $J = 0$ , other selection rules are operative. In such a case, for electric dipole transitions,  $\Delta|J| = 2, 4$ , or  $6$ . We observe that the presence of an inversion center opens up the possibility to tune the emission spectrum to a small extent. For  $\text{Eu}^{3+}$  with excited state  ${}^5\text{D}_0$ , the emission can be tuned from orange (590 nm, with inversion symmetry,  ${}^5\text{D}_0 \rightarrow {}^7\text{F}_1$  transition) to red (610 nm, without inversion symmetry,  ${}^5\text{D}_0 \rightarrow {}^7\text{F}_2$  transition). More generally, these effects can be described by the Judd-Ofelt theory [12,13]. As a function of three parameters, all possible spectra can be calculated. However, a direct coupling to the chemical environment is lacking. Nevertheless, such calculations are useful. Apart from being able to calculate the relative intensities, these calculations can also be used to calculate subsequent optical transitions, i.e. quantum cutters. For  $\text{Pr}^{3+}$ , in principle a quantum efficiency of 198 % can be obtained in the visible. The same kind of calculation has shown that for  $\text{Tm}^{3+}$ , no quantum cutter, a yield of two visible photons can be obtained [14].

Finally, in the case of donor-acceptor pair luminescence, both the donors and the acceptors and the magnitude of the band gap strongly influence the spectral position of the emission color to be obtained.  $\text{ZnS}:\text{Ag}$  and  $\text{ZnS}:\text{Cu,Au}$  (blue- and green-emitting phosphors, respectively, nicely illustrate this).

### 1.10

#### Energy Efficiency Considerations of Important Luminescent Devices

As argued above, in general, the luminescent materials applied operate at physical limits in terms of absorption of the exciting radiation and the quantum efficiency (number of visible photons generated divided by the number of photons absorbed) with which luminescence is generated. In cathode ray tubes, the energy efficiency of the phosphors used is at maximum (up to about 25 %, see above), and the quantum efficiency of the luminescent centers is almost 100 %.

In plasma display panels, fluorescent lamps, and LEDs, the quantum efficiency amounts about 100 %, and the absorption coefficient is also very high. Nevertheless, the energy efficiency of luminescent devices is rather low (see Table 1.4) in which the energy loss is factorized. The phosphor energy loss factor in this table is mainly determined by the Stokes shift (the difference in photon energy of radiation absorbed and emitted). This results in energy loss, which can be significant even when the quantum efficiency is 100 %.

We observe that, although the phosphors operate at physical limits, nevertheless the energy efficiency of the devices is rather low, especially in display applications.

Finally, Table 1.5 gives a survey of luminescent materials with popular applications.

### 1.11

#### Luminescence Quantum Yield and Quenching Processes

In this section, we deal with energy loss processes, to throw some light on the question why all phosphors do not have a quantum efficiency of unity and what the loss processes are. We base this discussion on Eq. (26). We also briefly discuss degradation processes in luminescent materials, which quite frequently occur during the operation of devices utilizing phosphors and which have a negative effect on the performance of such devices. The influence on device performance can be considerable, especially in case of

**Tab. 1.4** Energy efficiencies of important luminescent devices and a breakdown into the most important energy loss factors.

Device	Cathode ray tube	Plasma display panel	Fluorescent lamp	Phosphor-converted LED lamp
Energy efficiency (%)	1–2	2	Straight fluorescent: 25 Compact: 15	50
Major energy loss factors (%)	Shadow mask: 70–90 Phosphors: 80 Deflection yoke: 50	Discharge: 90 Phosphors: 70	Phosphors: 55 Discharge: 30 (Straight) Discharge: 40 (Compact)	LED: 40 Phosphors: 25

Tab. 1.5 Prominent phosphors and their applications.

Emission color	Application			
	Cathode ray tubes and projection television tubes (PTV)	Plasma display panels	Fluorescent lamps	X-ray detectors
UV			Ba <sub>2</sub> SiO <sub>5</sub> :Pb <sup>2+</sup> (sun tanning) CeMgAl <sub>11</sub> O <sub>19</sub> (sun tanning) LaPO <sub>4</sub> :Ce <sup>3+</sup> (sun tanning) SrB <sub>4</sub> O <sub>7</sub> :Eu <sup>2+</sup> (sun tanning, photo copiers)	
Blue	ZnS:Ag <sup>+</sup> ,Cl <sup>-</sup> ZnS:Ag <sup>+</sup> ,Al <sup>3+</sup>	BaMgAl <sub>10</sub> O <sub>17</sub> :Eu <sup>2+</sup>	BaMgAl <sub>10</sub> O <sub>17</sub> :Eu <sup>2+</sup> Sr <sub>4</sub> Al <sub>14</sub> O <sub>25</sub> :Eu <sup>2+</sup> Sr <sub>5</sub> (PO <sub>4</sub> ) <sub>3</sub> Cl:Eu <sup>2+</sup>	NaI:Tl <sup>+</sup> Ba(F,Br):Eu <sup>2+</sup> (storage phosphor) LaBr <sub>3</sub> :Ce <sup>3+</sup> Bi <sub>4</sub> Ce <sub>3</sub> O <sub>12</sub> Gd <sub>2</sub> SiO <sub>5</sub> :Ce <sup>3+</sup> Lu <sub>2</sub> SiO <sub>5</sub> :Ce <sup>3+</sup> LuAlO <sub>3</sub> :Ce <sup>3+</sup> YTaO <sub>4</sub> :Nb <sup>5+</sup>
Green	ZnS:Cu <sup>+</sup> ,Au <sup>+</sup> ,Al <sup>3+</sup> ZnS:Cu <sup>+</sup> ,Al <sup>3+</sup> Zn <sub>2</sub> SiO <sub>4</sub> :Mn <sup>2+</sup> (PTV) Y <sub>2</sub> SiO <sub>5</sub> :Tb <sup>3+</sup> (PTV) InBO <sub>3</sub> :Tb <sup>3+</sup> (PTV) LaOCl:Tb <sup>3+</sup> (PTV)	(Y,Gd)BO <sub>3</sub> :Tb BaAl <sub>12</sub> O <sub>19</sub> :Mn <sup>2+</sup> Zn <sub>2</sub> SiO <sub>4</sub> :Mn <sup>2+</sup> BaMgAl <sub>10</sub> O <sub>17</sub> :Eu <sup>2+</sup> ,Mn <sup>2+</sup>	GdMgB <sub>5</sub> O <sub>10</sub> :Ce <sup>3+</sup> ,Tb <sup>3+</sup> LaPO <sub>4</sub> :Ce <sup>3+</sup> ,Tb <sup>3+</sup> CeMgAl <sub>11</sub> O <sub>19</sub> :Tb <sup>3+</sup> Zn <sub>2</sub> SiO <sub>4</sub> :Mn <sup>2+</sup>	CsI:Tl <sup>+</sup> Gd <sub>2</sub> O <sub>3</sub> :Tb <sup>3+</sup> Gd <sub>2</sub> O <sub>3</sub> :Pr <sup>3+</sup>
Yellow			Y <sub>3</sub> Al <sub>5</sub> O <sub>12</sub> :Ce <sup>3+</sup>	(Y,Cd) <sub>3</sub> Al <sub>5</sub> O <sub>12</sub> :Ce <sup>3+</sup>
Red	Y <sub>2</sub> O <sub>3</sub> :Eu <sup>3+</sup> Y <sub>2</sub> O <sub>3</sub> :Eu (PTV)	Y <sub>2</sub> O <sub>3</sub> :Eu <sup>3+</sup> (Y,Gd)(P,V)O <sub>4</sub> :Eu <sup>3+</sup>	Y <sub>2</sub> O <sub>3</sub> :Eu <sup>3+</sup>	(Y,Gd) <sub>2</sub> O <sub>3</sub> :Eu <sup>3+</sup> , Pr <sup>3+</sup>
White	ZnS:Ag <sup>+</sup> + (Zn,Cd)S:Ag <sup>+</sup>		Ca <sub>5</sub> (PO <sub>4</sub> ) <sub>3</sub> (F,Cl):Sb <sup>3+</sup> ,Mn <sup>2+</sup>	CaS:Eu

cathode ray tubes, where phosphor degradation can contribute to an efficiency loss up to 30–50% during the operational lifetime. In fluorescent lamps, the maintenance of the phosphors is in general much better, and the efficiency loss over the operational lifetime can be less than 10%.

Looking at the expression in Eq. (26), we distinguish the following loss processes:

1. The absorbed energy does not reach the luminescent ions ( $\eta_i$ ).
2. The absorbed energy reaches the luminescent ions but there are nonradiative channels to the ground state ( $\eta_{act}$ ).
3. The luminescence generated is absorbed by the luminescent material ( $\eta_{esc}$ ).

In what follows, the underlying mechanisms will be treated in more detail.

### 1.11.1

#### **The Energy does not Reach the Luminescent Ion**

When there is more than one origin of optical absorption at the wavelength at which the excitation takes place, the quantum efficiency can be less than unity, even if the ion showing luminescence has a quantum efficiency of one. This is, e.g., the case if both the luminescent ion and the host lattice show optical absorption at the excitation wavelength, or the energy transfer probability of the host lattice to the luminescent ions is smaller than unity. Comparing the absorption or reflection spectra with the excitation spectra can disentangle the different contributions to the absorption.

Degradation of luminescent materials can be due to creation of additional absorption centers in the spectral range where the activators or sensitizers also absorb.

### 1.11.2

#### **The Absorbed Energy Reaches the Luminescent Ion but there are Nonradiative Channels to the Ground State**

The transition rate (units  $s^{-1}$ ) is given by  $k$ . If only emission occurs,  $k$  is written as  $k_r$ . If the transition involves radiative and nonradiative contributions,  $k$  is written as

$$k = k_r + k_{nr} \quad (34)$$

We observe that  $k$  increases in the case of nonradiative contributions to the transition rate. For this reason, the emission decay time (being  $1/k$ ) decreases in such cases. Using this expression, it is easily shown that the quantum yield can be determined by measuring the decay time ( $\tau$ ) if the decay time without nonradiative transitions ( $\tau_0$ ) is known:

$$QE = \tau/\tau_0 \quad (35)$$

The proof of this equation is left to the reader.

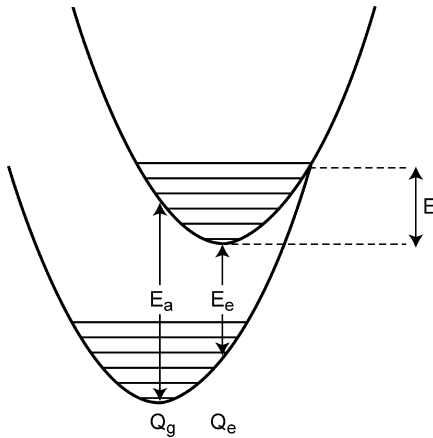


**Fig. 1.18** Crossing of parabolas describing ground and excited states, leading to thermal quenching characterized by the activation energy  $E$ .

Very frequently, the luminescent ion can reach the ground state via thermal quenching (see Fig. 1.18). This is the case when the excited state and the ground state energy curves cross at an energy which is thermally accessible from the relaxed excited state. For this reason, this process is called thermal quenching. Using the rate equations again, and assuming that the nonradiative rate  $k_{nr}$  can be written as

$$k_{nr} = A \cdot \exp(-E/kT) \quad (36)$$

in which  $A$  is a constant (units  $s^{-1}$ ) and  $E$  is the energy difference between the energy of the relaxed excited state and the energy at which the ground and excited states cross (Fig. 1.18).

The quantum efficiency is given by

$$QE = 1/(1 + C \cdot \exp(-E/kT)) \quad (37)$$

in which  $C$  is a dimensionless constant.

We observe that an increase in temperature results in a lower value for the quantum efficiency. The energy involved in the thermal quenching process is easily determined by measuring the decay time of quantum efficiency as a function of the temperature.

Of course, the elementary treatment leading to Eq. (37) describes quenching due to any thermally activated process, e.g., also thermal quenching due to photoionization. In this process, excited activator ions ionize thermally activated. This process is very important in, e.g., scintillators.

Another quenching process is related to energy transfer. If the concentration of luminescent ions chosen is too high, energy transfer occurs over the luminescent

ions until the energy reaches a center where a nonradiative transition occurs. Two remarks have to be made here:

- Energy transfer underlies sensitization schemes, in which case energy transfer is a useful process. Though the sensitizer emission is quenched, the activator emission appears. This allows practical application of sensitization schemes.
- In general the centers for nonradiative recombination are not known. In many cases, therefore, the possibility to increase the concentration of luminescent ions is limited. The mechanism leading to quantum yield loss is called concentration quenching. Whether or not this mechanism takes place can be easily deduced by investigating the quantum efficiency or the decay time of the emission as a function of the activator concentration.

Please note that a large difference between absorption and emission wavelength (Stokes shift) reduces energy transfer and therefore concentration quenching. On the other hand, a very large Stokes shift increases the probability for thermal quenching, as the ground state parabola will cross the excited state parabola at a lower energy, allowing the ground state parabola to be reached without emission of a photon. This is a direct consequence of the quadratic dependence of the potential energy of the electronic states on the metal-ligand distance, as the reader can easily verify. For the same reason, thermal quenching becomes less probable when the emission energy increases.

Degradation of luminescent materials can be due to additional centers to which energy can be transferred, without efficient photon generation by these centers (killing centers, killers, centers for nonradiative recombination). Such centers can be, e.g., vacancies generated as a consequence of the operation of the device or sensitizer or activator ions that have changed their valence during operation of the device.

### 1.11.3

#### **The Luminescence Generated is Absorbed by the Luminescent Material**

Finally, even if all the absorbed energy is converted into emission, the quantum efficiency is not necessarily one. For example, this is the case when the host lattice itself shows optical absorption in the spectral range where emission occurs. This is easily determined by measuring the absorption or reflection spectra of the host material.

Self-absorption is also an important loss factor in luminescent structures which do not effectively scatter the luminescence light. This is the case, e.g., in organic or inorganic LEDs, where trapping of light in the luminescent structure, followed by absorption of the light emitted in the luminescent material, strongly reduces the light output. In such a case, additional scattering, e.g., by applying scattering layers to such structures or applying photonic structures such that light is generated in desired directions only, can be a way out.

Degradation of luminescent materials (resulting in a loss of photon generating efficiency) is often due to additional absorption bands which are not present in the virgin material. Absorption or reflection spectroscopy therefore are important techniques in understanding the physical origin of light generation losses of phosphors.

## 1.12

### Acknowledgement

Considerable parts of the contents of this chapter (text and figures) have appeared in Refs. [15–17]. With kind permission of Springer Science and Business Media and World Scientific.

### References

- 1 Förster, T. (1951) *Fluoreszenz Organischer Verbindungen*, Vandenhoeck, Ruprecht, Göttingen.
- 2 Förster, T. (1959) *Disc. Faraday Soc.*, **27**, 7.
- 3 Förster, T. *Ann. Phys.*, (1948) **2**, 55.
- 4 DiBartolo, B. (1984) Energy Transfer Processes in Condensed Matter, in *NATO ASI Series, Series B: Physics*, (ed. B. DiBartolo) **114**, Plenum Press, New York.
- 5 Dexter, D. L. (1953) *J. Chem. Phys.*, **21**, 836.
- 6 Stevels, A. L. N. and Verstegen, J. M. P. J. (1976) *J. Lumin.*, **14**, 207.
- 7 Verstegen, J. M. P. J., Sommerdijk, J. L., Verriet, J. G. (1973) *J. Lumin.*, **6**, 425.
- 8 Soules, T. F., Bateman, R.L., Hewes, R. L., Kreidler, E. R. (1973) *Phys. Rev.*, **B7**, 1657.
- 9 Robbins, D. J. (1980) *J. Electrochem. Soc.*, **127**, 2694.
- 10 Bartram, R. H., Lempicki, A. (1996) *J. Lumin.*, **69**, 225.
- 11 Meijerink, A., Nuyten, J., Blasse, G. (1989) *J. Lum.*, **44**, 19.
- 12 Ofelt, G. S. (1962) *J. Chem. Phys.*, **37**, 511.
- 13 Judd, B. R. (1962) *Phys. Rev.*, **127**, 750.
- 14 Nieuwesteeg, K. J. B. M. (1989) *Philips J. Res.*, **44**, 383.
- 15 Ronda, C. R. (1997) *Spectroscopy, Dynamics of Collective Excitation in Solids*, in *NATO ASI Series, Series B, Physics*, (eds. B.DiBartolo and S. Kyrkos) **356**, Plenum Press, New York, 339–373.
- 16 Ronda, C. R. *Frontiers in Optical Spectroscopy, NATO Science Series II Mathematics, Physics, Chemistry*, (eds B. DiBartolo and O. Forte), Kluwer Academic Publishers, Dordrecht, Boston, London, **168**, 359–392.
- 17 Ronda, C. R. *Advances in Energy Transfer Processes, World Scientific, the Science and Culture Series* (eds. B. DiBartolo and X. Chen), World Scientific, New Jersey, London, Singapore, Hong Kong, 377–408.